Argand Diagrams, Cross-Section Behavior, and Regge Poles

NAOHIKO MASUDA
Department of Physics, Louisiana State University, Baton Rouge, Louisiana 70803
(Received 6 October 1969)

Schmid's problem on the interpretation of the anticlockwise Argand diagram obtained from Regge-pole exchanges as the direct-channel resonance is studied. It is shown in the idealized models that the anticlockwise Argand diagram alone cannot guarantee the existence of a resonance, and that it is absolutely necessary to compute the cross section in order to establish the existence of a resonance. The partial-wave projection of the Regge-pole exchanges in pion-nucleon scattering is performed. The Argand diagram, real part of phase shift, absorption factor, partial-wave total cross section σ^{tot}, elastic cross section σ^{el}, $k^2\sigma^{tot}$, and $k^2\sigma^{el}$ are computed. It is found that all σ^{tot} and σ^{el} have no cross-section peak at all, despite the existence of the anticlockwise Argand loops in certain partial waves. They show only the monotonically decreasing behavior characteristic of the Regge-pole model as energy increases, except in the unitarity-violating low-energy region. The above facts indicate that the variation of the anticlockwise Argand loop with respect to energy is too weak to produce a cross-section peak by overcoming the variation of the barrier factor $1/k^2$ in σ^{tot} and σ^{el}. It is concluded that Schmid's interpretation is incorrect. Several physical implications of this result are discussed.

I. INTRODUCTION

A RESONANCE, as described by a Breit-Wigner one-level formula, draws an anticlockwise Argand loop as a function of energy. From the resemblance of the shapes of the Argand diagrams, Schmid[1] proposed that the anticlockwise Argand loop obtained by the partial-wave projection of Regge-pole exchanges should be interpreted as a direct-channel resonance. From this, Schmid claimed that the so-called duality principle[2] actually holds between Regge-pole exchanges in crossed channels and direct-channel resonances.

Since then a number of papers[3–11] on this problem have appeared. Although all papers confirm the existence of such anticlockwise Argand loops as claimed by Schmid, it seems that no one has been able to give a definite answer on whether the anticlockwise Argand loops obtained from the partial-wave projection of Regge-pole exchanges really indicate the existence of resonances or not. Thus, one of the bases of the duality concept is still questionable.

On the other hand, Lichtenberg, Newton, and Predazzi[12] have recently shown that the Veneziano formula, which had been supposed to satisfy the duality principle, is actually equivalent to the interference model; and they cast serious doubt on the existence of a scattering amplitude which satisfies the duality principle along with the other fundamental requirements, such as crossing symmetry and Regge behavior.

In view of these circumstances, it is important to clarify whether Schmid's interpretation is correct or not.

In this paper, from the general behavior of the scattering amplitude such as that of the real part of the phase shift, the absorption factor, and the cross section, we will show that any type of cross-section behavior, such as dip, flat, resonance, and others, can produce the anticlockwise Argand loops depending on the details of the behavior of the real part of the phase shift and the absorption factor. That is, the anticlockwise Argand loop alone cannot guarantee the existence of a resonance. Therefore, it is absolutely necessary to compute the partial-wave cross section and to detect the cross-section peak in order to justify Schmid's interpretation. All papers[1,3–11] so far published on this problem produced the anticlockwise Argand loops but failed to test the cross-section behavior. Therefore, it is naturally understood why no definite answer on this problem has yet been obtained.

Bearing in mind the above remarks, we perform the partial-wave projection of Regge-pole exchanges in pion-nucleon scattering and show that several partial-wave amplitudes produce anticlockwise Argand loops similar to that of a Breit-Wigner one-level formula, but that the cross sections of all partial-wave amplitudes give neither a resonancelike peak nor dip but only the smooth behavior characteristic of the Regge-pole model. From this fact, it is concluded that Schmid's interpretation of the anticlockwise Argand loops, obtained from partial-wave projection of the Regge-pole exchanges as resonances, is wrong, and also that the statement of Collins *et al.*[6] that the resonance partial-

[1] C. Schmid, Phys. Rev. Letters **20**, 689 (1968).
[2] R. Dolen, D. Horn, and C. Schmid, Phys. Rev. **166**, 1779 (1968).
[3] H. R. Rubinstein, A. Schwimmer, G. Veneziano, and M. A. Virasoro, Phys. Rev. Letters **21**, 491 (1968).
[4] M. Kugler, Phys. Rev. **180**, 1538 (1969); Phys. Rev. Letters **21**, 570 (1968).
[5] Y. Kohsaka, O. Miyamura, F. Takagi, and K. Itabashi, Nuovo Cimento Letters **1**, 404 (1969).
[6] P. D. B. Collins, R. C. Johnson, and E. J. Squires, Phys. Letters **27B**, 23 (1968).
[7] V. A. Alessandrini and E. J. Squires, Phys. Letters **27B**, 300 (1968).
[8] V. A. Alessandrini, P. G. O. Freund, R. Oehme, and E. J. Squires, Phys. Letters **27B**, 456 (1968).
[9] V. A. Alessandrini, D. Amati, and E. J. Squires, Phys. Letters **27B**, 463 (1968).
[10] N. R. Lipshutz, Phys. Rev. **181**, 1972 (1969).
[11] C. B. Chiu and A. Kotanski, Nucl. Phys. **B7**, 615 (1968).
[12] D. B. Lichtenberg, R. G. Newton, and E. Predazzi, Phys. Rev. Letters **22**, 1215 (1969). See also R. Jengo, Phys. Letters **28B**, 606 (1969); R. W. Childers, Phys. Rev. Letters **23**, 357 (1969).

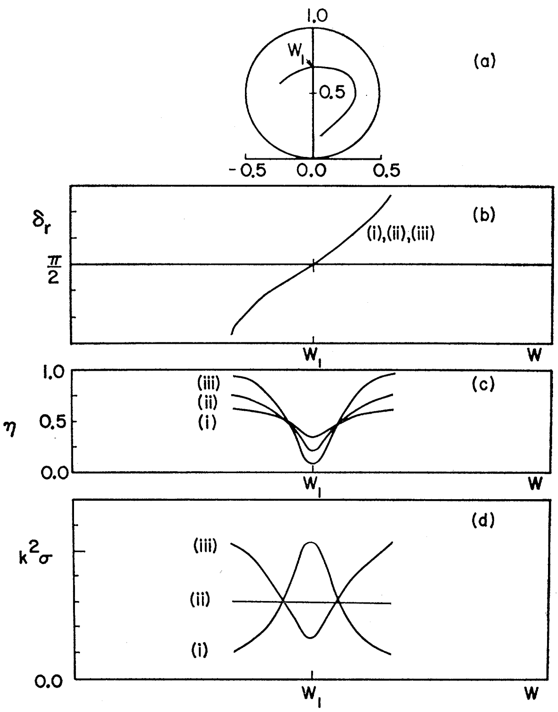

FIG. 1. Example of typical behavior of the $\delta_r(W)$, $\eta(W)$, and $k^2\sigma_{Jl}(W)$ associated with the anticlockwise Argand loop (a) in which $\delta_r(W_1)=\frac{1}{2}\pi$ and $[d\delta_r(W)/dW]_{W=W_1}>0$. (i), (ii), and (iii) in (b), (c), and (d) correspond to a peak, a flat behavior, and a dip of $k^2\sigma_{Jl}^{\text{tot}}(W)$ $[k^2\sigma_{Jl}^{\text{el}}(W)]$ according to Eqs. (22a), (22b), and (22c) [(24a), (24b), and (24c)], respectively.

wave amplitudes obtained as above should be canceled by the other partial-wave amplitudes, so as to give a smooth behavior to the total Regge-pole exchange amplitudes, is also incorrect. In order to demonstrate this fact more clearly, we show several Argand diagrams which do not have anticlockwise loops, and their corresponding cross-section behavior. All partial-wave cross sections obtained from Regge-pole exchanges produce qualitatively the same behavior.

In Sec. II we discuss in the idealized models the general behavior of the real part of the phase shift, the absorption factor, and the cross section of a partial-wave amplitude which produces the anticlockwise Argand loop. In this paper we define the Argand locus which passes from the right-hand half-circle to the left-hand half-circle with increasing energy as the anticlockwise Argand loop, independent of its exact shape. This general assumption is necessary because the anticlockwise loops in the partial-wave amplitudes with high inelasticities are often distorted ones, and the energy dependence of Argand loops obtained from Regge-pole exchanges is extremely weak, as will be shown in Sec. III.

We find the relationship between the behavior of the real part of the phase shift and the absorption factor of an amplitude with an anticlockwise Argand loop to have a peak, flat behavior, and dip in $k^2\sigma^{\text{tot}}$ and $k^2\sigma^{\text{el}}$.

In Sec. III, we perform the partial-wave projection of Regge-pole exchanges for pion-nucleon scattering. Several partial-wave amplitudes which draw anticlockwise Argand loops are found. We show the Argand diagrams, the real parts of the phase shifts, the absorption factors, σ^{tot}, σ^{el}, $k^2\sigma^{\text{tot}}$, and $k^2\sigma^{\text{el}}$ for these partial-wave amplitudes and explain why these partial-wave amplitudes should not be interpreted as direct-channel resonances.

In Sec. IV, we discuss several physical implications of our conclusion.

II. ARGAND DIAGRAMS, PHASE SHIFTS, AND CROSS SECTIONS

In this section, we discuss in the idealized models the general relationship among the real part of the phase shift, the absorption factor, and the cross section. The lth partial-wave amplitude with total spin J for a definite isotopic eigenstate is defined as

$$f_{Jl}(W)=\frac{\eta e^{2i\delta_r}-1}{2ik}, \tag{1}$$

where the absorption factor η is given by

$$\eta=e^{-2\delta_i}. \tag{2}$$

In Eqs. (1) and (2), W and k are the c.m. energy and three-momentum, respectively, and δ_r and δ_i are the real and imaginary parts of the phase shift, respectively. We omit the isotopic suffix in Eq. (1). Also omitted are the total-spin suffix J and the partial-wave suffix l in the δ_r, δ_i, and η.

For convenience in drawing the Argand diagram in a unit circle, we define $\text{Re}a_{Jl}(W)$ and $\text{Im}a_{Jl}$ from Eq. (1) as

$$\text{Re}a_{Jl}(W)=\text{Re}[kf_{Jl}(W)]=\tfrac{1}{2}\eta\sin 2\delta_r \tag{3}$$

and

$$\text{Im}a_{Jl}(W)=\text{Im}[kf_{Jl}(W)]=\tfrac{1}{2}(1-\eta\cos 2\delta_r). \tag{4}$$

The partial-wave total and elastic cross sections are given in terms of δ_r and η as

$$\sigma_{Jl}^{\text{tot}}(W)=\frac{2\pi(J+\frac{1}{2})}{k^2}(1-\eta\cos 2\delta_r) \tag{5}$$

and

$$\sigma_{Jl}^{\text{el}}(W)=\frac{J+\frac{1}{2}}{k^2}(1+\eta^2-2\eta\cos 2\delta_r). \tag{6}$$

In order to discuss the general properties of the scattering amplitudes, including the resonance amplitude as a special case, we first assume a Breit-Wigner one-level formula for $f_{Jl}(W)$:

$$f_{Jl}(W)=\frac{1}{k}\frac{\frac{1}{2}\Gamma_{\text{el}}}{W_1-W-\frac{1}{2}i\Gamma}, \tag{7}$$

where W_1, Γ, and Γ_{el} are the resonance energy, total decay width, and elastic decay width, respectively. From Eq. (7), we obtain the partial-wave total and elastic cross sections for a Briet-Wigner-type resonance as

$$\sigma_{Jl}^{\mathrm{tot}}(W)=\frac{2\pi(J+\frac{1}{2})}{k^2}\frac{\frac{1}{4}\Gamma\Gamma_{\mathrm{el}}}{(W_1-W)^2+\frac{1}{4}\Gamma^2} \tag{8}$$

and

$$\sigma_{Jl}^{\mathrm{el}}(W)=\frac{\pi(J+\frac{1}{2})}{k^2}\frac{\frac{1}{4}\Gamma_{\mathrm{el}}^2}{(W_1-W)^2+\frac{1}{4}\Gamma^2}. \tag{9}$$

It is evident from Eqs. (8) and (9) that if a Breit-Wigner-type resonance exists in a certain partial-wave amplitude, both $\sigma_{Jl}^{\mathrm{tot}}(W)$ and $\sigma_{Jl}^{\mathrm{el}}(W)$ should have peaks between the elastic threshold and W_1, unless W_1 is very close to the elastic threshold. This fact should be emphasized in connection with the discussion of the partial-wave projection of Regge-pole exchanges in Sec. III. $k^2\sigma_{Jl}^{\mathrm{tot}}(W)$ and $k^2\sigma_{Jl}^{\mathrm{el}}(W)$ should, of course, have peaks at $W=W_1$.

From Eq. (7), we obtain

$$\mathrm{Re}a_{Jl}(W)=\frac{\frac{1}{2}\Gamma_{\mathrm{el}}(W_1-W)}{(W_1-W)^2+\frac{1}{4}\Gamma^2} \tag{10}$$

and

$$\mathrm{Im}a_{Jl}(W)=\frac{\frac{1}{4}\Gamma\Gamma_{\mathrm{el}}}{(W_1-W)^2+\frac{1}{4}\Gamma^2}. \tag{11}$$

As W increases, Eqs. (10) and (11) draw anticlockwise loops as is shown in Fig. 1(a) when $\Gamma_{\mathrm{el}}/\Gamma>0.5$ and as in Fig. 2(a) when $\Gamma_{\mathrm{el}}/\Gamma<0.5$. As is stated in Sec. I, *we assume that the Argand loop which passes through the* $\mathrm{Re}a_{Jl}(W)=0$ *axis from the right-hand half-circle to the left-hand half-circle with increasing energy is the anticlockwise Argand loop.* This broad definition of the anticlockwise Argand loop is necessary because an amplitude with a very weak energy dependence as in Sec. III can draw only a small segment of the anticlockwise loop in the energy intervals of about the total decay widths of the experimentally observed pion-nucleon resonances (0.1–0.5 GeV). Also we assume that the value $W=W_1$ at which $\mathrm{Re}a_{Jl}(W)=0$ occurs is the resonance energy if the cross section has a Breit-Wigner-type peak. Of course, one may identify the maximum point of $\mathrm{Im}a_{Jl}(W)$ as the resonance energy even when the Argand locus does not pass through the $\mathrm{Re}a_{Jl}(W)=0$ axis (see, for example, the Argand diagram of the S_{31} state in pion-nucleon scattering, Fig. 9 of the paper by Bareyre *et al.*[13]). However, in this case, if we want to express this peak with a Breit-Wigner formula, we must add the background effect (attractive or repulsive) to the Breit-Wigner amplitude. Thus, only the interference model[14,15] can describe this amplitude. When we discuss Schmid's interpretation of the Argand loop obtained from Regge poles and its implications for the duality principle, the distorted anticlockwise loop in which the resonance energy has no close relation to the $\mathrm{Re}a_{Jl}(W)=0$ is not a suitable one. Therefore, we concentrate on the Argand diagram whose locus passes through the $\mathrm{Re}a_{Jl}(W)=0$ axis.

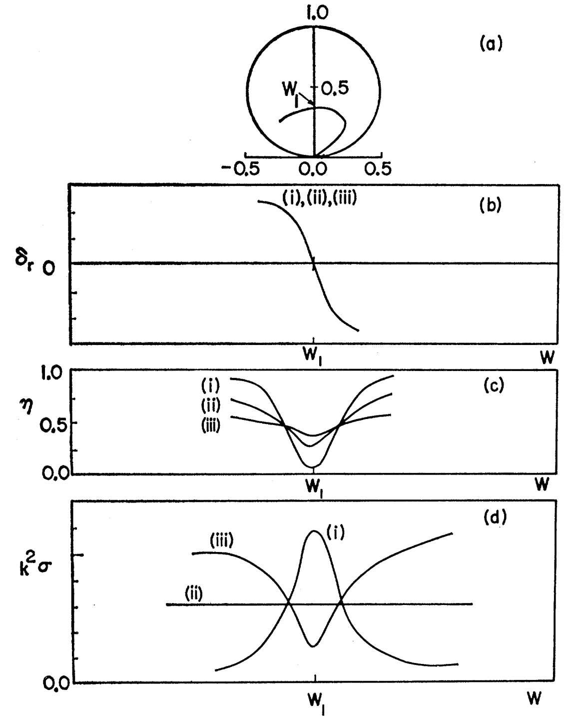

FIG. 2. Example of typical behavior of the $\delta_r(W)$, $\eta(W)$, and $k^2\sigma_{Jl}(W)$ associated with the anticlockwise Argand loop (a) in which $\delta_r(W_1)=0$ and $[d\delta_r(W)/dW]_{W=W_1}<0$. (i), (ii), and (iii) in (b), (c), and (d) correspond to a peak, a flat behavior, and a dip of $k^2\sigma_{Jl}^{\mathrm{tot}}(W)$ $[k^2\sigma_{Jl}^{\mathrm{el}}(W)]$ according to Eqs. (26a), (26b), and (26c) [(27a), (27b), and (27c)], respectively.

In order to relate $W=W_1$ in Figs. 1(a) and 2(a) with the real part of the phase shift, we use another expression for the partial-wave amplitude:

$$a_{Jl}(W)=kf_{Jl}(W)=\frac{1}{\cot(\delta_r+i\delta_i)-i}. \tag{12}$$

Comparing Eq. (12) with Eq. (7), we obtain the value of the real part of the phase shift and its first derivative at the resonance energy from the following equation:

$$\mathrm{Re}a_{Jl}^{-1}(W)=\frac{2\sin\delta_r\cos\delta_r}{\cosh2\delta_i-\cos2\delta_r}=0. \tag{13}$$

[13] P. Bareyre, C. Bricman, and G. Villet, Phys. Rev. **165**, 1730 (1968).

[14] V. Barger and D. Cline, Phys. Rev. **155**, 1792 (1967).

[15] It is known that Barger and Cline's original interference model (Ref. 14) violates the unitarity limit. In order to avoid this trouble, we have to construct the resonating partial-wave amplitude in the presence of background effects as the summation of the background amplitude and the Breit-Wigner resonance amplitude with complex phase factor due to background effects. The above interference formula has been well known in nonrelativistic scattering theory. See N. Masuda [report, 1969 (unpublished)] for the application of this model to pion-nucleon scattering.

From Eq. (13) we find two kinds of resonances corresponding to the following two different kinds of phase-shift behavior:

case (1):

$$\delta_r(W_1)=\tfrac{1}{2}\pi \quad \text{and} \quad \left.\frac{d\delta_r(W)}{dW}\right|_{W=W_1}>0 \tag{14}$$

and

case (2):

$$\delta_r(W_1)=0 \quad \text{and} \quad \left.\frac{d\delta_r(W)}{dW}\right|_{W=W_1}<0. \tag{15}$$

From Eqs. (3) and (4), we identify Eq. (14) with the anticlockwise Argand loop in Fig. 1(a), and Eq. (15) with the anticlockwise Argand loop in Fig. 2(a). That is, if a partial-wave amplitude has a resonance at $W=W_1$, we can summarize several properties in the following way:

(1) Fig. 1(a):

$$\Gamma_{\mathrm{el}}/\Gamma>0.5\,, \quad \delta_r(W_1)=\tfrac{1}{2}\pi\,, \quad \text{and} \quad \left.\frac{d\delta_r(W)}{dW}\right|_{W=W_1}>0 \tag{16}$$

and

(2) Fig. 2(a):

$$\Gamma_{\mathrm{el}}/\Gamma<0.5\,, \quad \delta_r(W_1)=0\,, \quad \text{and} \quad \left.\frac{d\delta_r(W)}{dW}\right|_{W=W_1}<0. \tag{17}$$

So far, we have discussed only the partial-wave amplitude in which a resonance exists. But our problem is to show that anticlockwise Argand loops such as in Figs. 1(a) and 2(a) do not necessarily mean the existence of a resonance. From Eqs. (3) and (4), it is easily understood that only Eq. (14) or (15) for the behavior of the real part of the phase shift is necessary to draw an anticlockwise Argand loop.

We assume the following linear forms of $\delta_r(W)$ as a function of energy near $\delta_r(W)=\frac{1}{2}\pi$ or $\delta_r(W)=0$:

case (1):

$$\delta_r(W)=a(W-W_1)+\tfrac{1}{2}\pi\,, \quad \text{where} \quad a>0 \tag{18}$$

and

case (2):

$$\delta_r(W)=a(W-W_1)\,, \quad \text{where} \quad a<0. \tag{19}$$

Using Eqs. (18) and (19), and restricting the cross-section behavior to cases symmetrical about $W=W_1$ (which include the Breit-Wigner resonance), we can show that the absorption factor $\eta(W)$ should also be symmetrical about $W=W_1$. For the simplest case, we assume the following form for $\eta(W)$:

$$\eta(W)=b(W-W_1)^2+c\,, \tag{20}$$

where $0.0\leq\eta(W)\leq1.0$ and $0.0\leq c\leq1.0$.

Equations (18) and (20) are the parametrizations for $\delta_r(W)$ and $\eta(W)$ with which the partial-wave amplitude draws an anticlockwise Argand loop similar to Fig. 1(a). The corresponding cross section may take any shape depending on a, b, and c.

Equations (19) and (20) are the parametrization for $\delta_r(W)$ and $\eta(W)$ with which the partial-wave amplitude draws an anticlockwise Argand loop similar to Fig. 2(a). Similarly, the corresponding cross section may take any shape depending on a, b, and c.

Next we obtain relations among the parameters a, b, and c in Eqs. (18)–(20) in order for the partial wave $k^2\sigma_{Jl}{}^{\mathrm{tot}}(W)$ or $k^2\sigma_{Jl}{}^{\mathrm{el}}(W)$ to have a peak, a flat behavior, and a dip.

Case (1): $k^2\sigma_{Jl}{}^{\mathrm{tot}}(W)$ with $\delta_r(W_1)=\frac{1}{2}\pi$ and $[d\delta_r(W)/dW]_{W=W_1}>0$.

By inserting Eqs. (18) and (20) into Eq. (5), we obtain

$$k^2\sigma_{Jl}{}^{\mathrm{tot}}(W)=2\pi(J+\tfrac{1}{2})\{1-[b(W-W_1)^2+c]\times\cos[2a(W-W_1)+\pi]\}\,. \tag{21}$$

From Eq. (21), we obtain the conditions for which $k^2\sigma_{Jl}{}^{\mathrm{tot}}(W)$ has a peak, a flat behavior, and a dip at $W=W_1$ as

$$\text{(i)} \quad \text{peak:} \quad b<2a^2c\,, \tag{22a}$$

$$\text{(ii)} \quad \text{flat behavior:} \quad b=2a^2c\,, \tag{22b}$$

and

$$\text{(iii)} \quad \text{dip:} \quad b>2a^2c\,. \tag{22c}$$

Case (1): $k^2\sigma_{Jl}{}^{\mathrm{el}}(W)$ with $\delta_r(W_1)=\frac{1}{2}\pi$ and $[d\delta_r(W)/dW]_{W=W_1}>0$.

By inserting Eqs. (18) and (20) into Eq. (6), we obtain

$$k^2\sigma_{Jl}{}^{\mathrm{el}}(W)=\pi(J+\tfrac{1}{2})\{1+[b(W-W_1)^2+c]^2-2[b(W-W_1)^2+c]\cos[2a(W-W_1)+\pi]\}\,. \tag{23}$$

From Eq. (23), we obtain the conditions for which $k^2\sigma_{Jl}{}^{\mathrm{el}}(W)$ has a peak, flat behavior, and a dip at $W=W_1$ as

$$\text{(i)} \quad \text{peak:} \quad b<2a^2c/(1+c)\,, \tag{24a}$$

$$\text{(ii)} \quad \text{flat behavior:} \quad b=2a^2c/(1+c)\,, \tag{24b}$$

and

$$\text{(iii)} \quad \text{dip:} \quad b>2a^2c/(1+c)\,. \tag{24c}$$

Comparing Eqs. (22a) and (24a) for the peaks of $k^2\sigma_{Jl}{}^{\mathrm{tot}}(W)$ and $k^2\sigma_{Jl}{}^{\mathrm{el}}(W)$, respectively, it is instructive to note that the existence of a maximum of $\mathrm{Im}a_{Jl}(W)$ in an anticlockwise Argand loop does not necessarily mean the existence of a Breit-Wigner-type resonance. Although the maximum of $\mathrm{Im}a_{Jl}(W)$ produces the peak in $k^2\sigma_{Jl}{}^{\mathrm{tot}}(W)$ $[=2\pi(J+\frac{1}{2})\mathrm{Im}a_{Jl}(W)]$, it does not necessarily produce the peak in $k^2\sigma_{Jl}{}^{\mathrm{el}}(W)$ $(=(J+\frac{1}{2})\times\{[\mathrm{Re}a_{Jl}(W)]^2+[\mathrm{Im}a_{Jl}(W)]^2\})$, because the condition (24a) for $k^2\sigma_{Jl}{}^{\mathrm{el}}(W)$ is stronger than the condition (22a) for $k^2\sigma_{Jl}{}^{\mathrm{tot}}(W)$. In this context, we stress that the automatic identification of a maximum in $\mathrm{Im}a_{Jl}(W)$

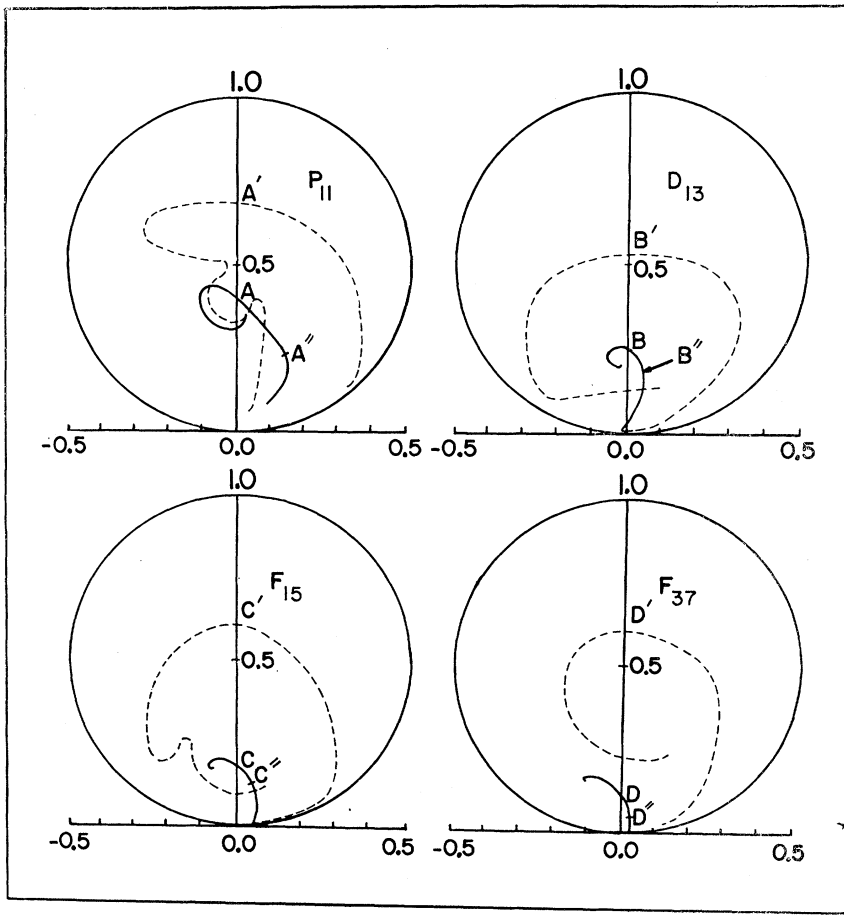

FIG. 3. Anticlockwise Argand loops. Straight lines are from the partial-wave projection of the Regge-pole exchanges in pion-nucleon scattering. The crossing points of loci through the $\mathrm{Re}a_{Jl}(W)=0$ axis are indicated by A, B, C, and D in the respective figures. At these points, $\delta_r(W)$ passes zero downward. Dashed lines are from Bareyre *et al.*'s phenomenological phase-shift analysis, Ref. 13. Crossing points of loci through the $\mathrm{Re}a_{Jl}(W)=0$ axis are indicated by A', B', C', and D' in the respective figures. At these points $\delta_r(W)$ passes 90° upward. Momentum regions of loops are the same as those of $\delta_r(W)$ and $\eta(W)$ in Figs. 4 and 5.

in an anticlockwise Argand diagram with a resonance in Refs. 1, 4–6, and 10 should be reexamined.

When a Breit-Wigner-type resonance exists, we can obtain the elastic decay width from Eqs. (7) and (12) as[16]

$$\Gamma_{\mathrm{el}}=2\cosh^2\delta_i \Big/ \frac{d\delta_r}{dW}\bigg|_{W=W_1}. \tag{25}$$

Illustrative examples are shown in Fig. 1.

Using Eqs. (5), (6), (19), and (20), we can obtain the conditions for which $k^2\sigma_{Jl}{}^{\mathrm{tot}}(W)$ or $k^2\sigma_{Jl}{}^{\mathrm{el}}(W)$ has a peak, a flat behavior, and a dip at $W=W_1$ in case (2), in the same manner as in case (1).

Case (2): $k^2\sigma_{Jl}{}^{\mathrm{tot}}(W)$ with $\delta_r(W_1)=0$ and $[d\delta_r(W)/dW]_{W=W_1}<0$.

The conditions are

(i) peak: $b>2a^2c$, (26a)

(ii) flat behavior: $b=2a^2c$, (26b)

and

(iii) dip: $b<2a^2c$. (26c)

Case (2): $k^2\sigma_{Jl}{}^{\mathrm{el}}(W)$ with $\delta_r(W_1)=0$ and $[d\delta_r(W)/dW]_{W=W_1}<0$.

The conditions are

(i) peak: $b>2a^2c/(1-c)$, (27a)

(ii) flat behavior: $b=2a^2c/(1-c)$, (27b)

and

(iii) dip: $b<2a^2c/(1-c)$. (27c)

Again, we note that from the conditions (26a) and (27a), the existence of the maximum of $\mathrm{Im}a_{Jl}(W)$ in an anticlockwise Argand loop does not necessarily imply the existence of a Breit-Wigner-type resonance, because although the maximum of $\mathrm{Im}a_{Jl}(W)$ indicates a peak in $k^2\sigma_{Jl}{}^{\mathrm{tot}}$, it does not necessarily indicate a peak in $k^2\sigma_{Jl}{}^{\mathrm{el}}(W)$. However, from Eqs. (8) and (9), if a Breit-Wigner-type resonance exists, both $k^2\sigma_{Jl}{}^{\mathrm{tot}}(W)$ and $k^2\sigma_{Jl}{}^{\mathrm{el}}(W)$ should have peaks.

If a Breit-Wigner-type resonance in case (2) exists, its elastic decay width can be obtained from Eqs. (7) and (12) as

$$\Gamma_{\mathrm{el}}=-2\sinh^2\delta_i \Big/ \frac{d\delta_r}{dW}\bigg|_{W=W_1}. \tag{28}$$

From the conditions (26a) and (27a) for the cross-section peaks in case (2), it is evident that only when the absorption factor sharply decreases about $W=W_1$

[16] Y. Fujii and M. Uehara, Progr. Theoret. Phys. (Kyoto) Suppl. 21, 138 (1962).

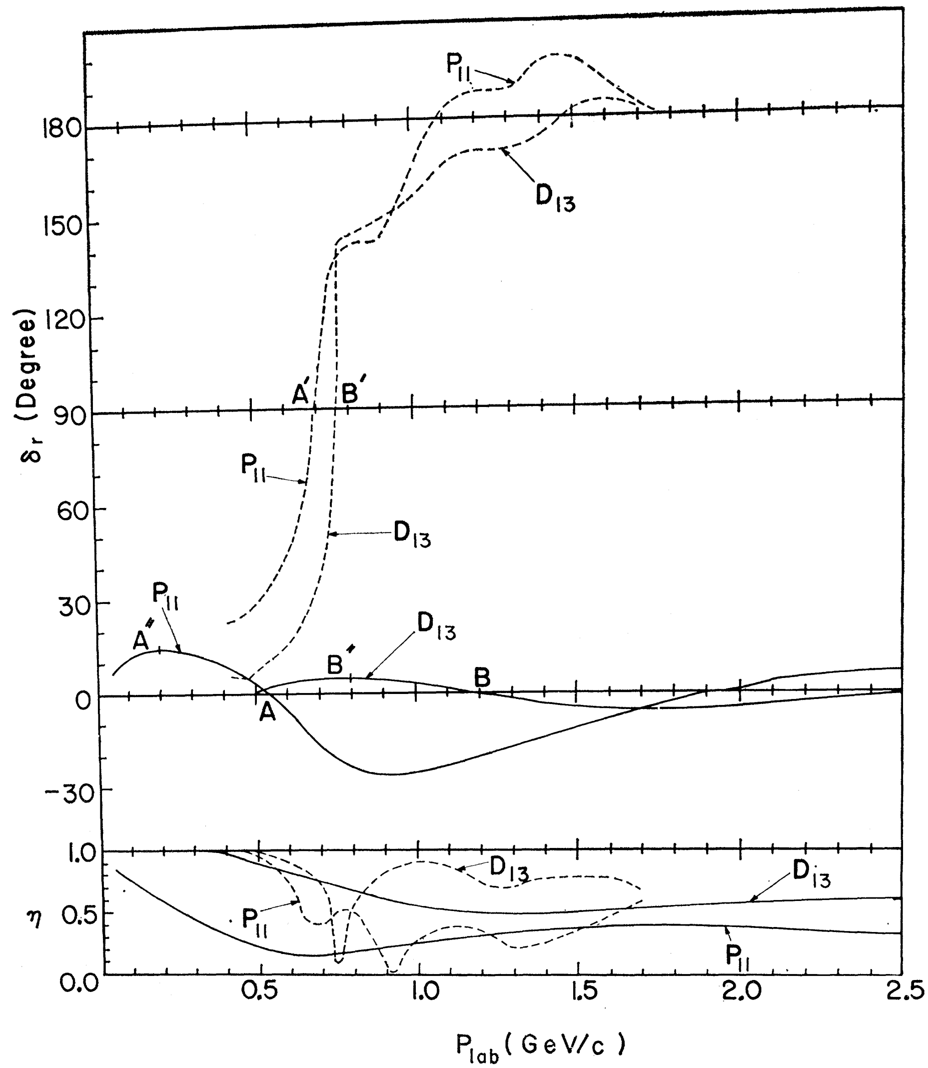

FIG. 4. Behavior of $\delta_r(W)$ and $\eta(W)$ in the P_{11} and D_{13} states. Straight lines are from the Regge-pole exchanges. Dashed lines are from Bareyre *et al.*, Ref. 13.

does the partial-wave amplitude have a resonance. Illustrative examples of case (2) are shown in Fig. 2.

Before concluding this section, we would like to emphasize again that the anticlockwise Argand loop alone cannot guarantee the existence of a resonance. It is necessary to compute the partial-wave total and elastic cross sections in order to establish the existence of a resonance. In this context we point out that all papers, including Schmid's original one, so far published on this problem failed to realize this fact. They produced only Argand diagrams. Therefore, both conclusions supporting and opposing Schmid's interpretation of partial-wave projection of Regge-pole exchanges should be reexamined in light of our conclusion. Since we derived Eqs. (25) and (28) from Eqs. (7) and (12), we can always identify the second-sheet pole near the unitarity cut with the existence of the Breit-Wigner-type cross-section peak.

Schmid[17] states that the relation of a second-sheet pole to the anticlockwise Argand loop obtained from the partial-wave projection of Regge-pole exchanges is not clear. However, if the partial-wave cross section shows a Breit-Wigner-type peak, then whatever its origin, it can be effectively expressed in terms of a second-sheet pole of the amplitude near the unitarity cut.

III. PARTIAL-WAVE PROJECTION OF REGGE-POLE EXCHANGE

In Sec. II we explained why the anticlockwise Argand loop alone cannot guarantee the existence of a resonance. We showed that when the Argand locus moves from the right-hand half-circle to the left-hand half-circle through the $\mathrm{Re}\,a_{Jl}(W)=0$ axis, the corresponding cross sections $k^2\sigma_{Jl}^{\mathrm{tot}}(W)$ and $k^2\sigma_{Jl}^{\mathrm{el}}(W)$ may exhibit a

[17] C. Schmid, Nuovo Cimento **61A**, 289 (1969).

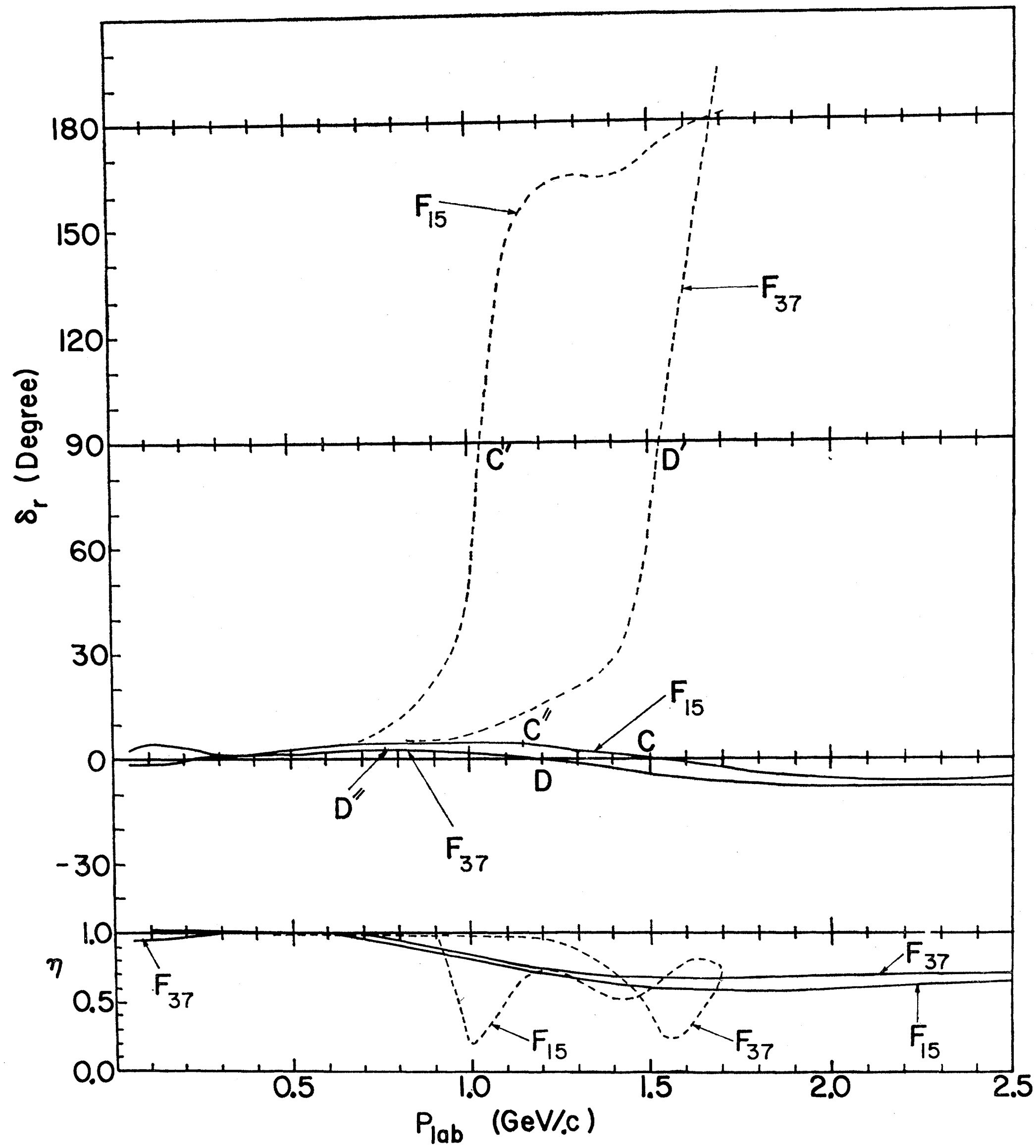

FIG. 5. Behavior of $\delta_r(W)$ and $\eta(W)$ in the F_{15} and F_{37} states. Straight and dashed lines mean the same as in Fig. 4.

resonance, a flat behavior, or a dip depending on the details of the energy dependence of $\delta_r(W)$ and $\eta(W)$.

In this section, we perform the partial-wave analysis of the Regge-pole exchanges for pion-nucleon scattering at intermediate energies, and test whether the anticlockwise Argand diagrams found in several partial waves actually show the partial-wave total and elastic cross-section maxima or not.

Our Regge-pole parameters are taken from Barger and Phillips[18] for the forward region ($0°\leq\theta\leq 90°$) and from Barger and Cline[19] for the backward regions ($90°<\theta\leq 180°$).

[18] V. Barger and R. J. N. Phillips, Phys. Rev. Letters 22, 116 (1969).

[19] V. Barger and D. Cline, Phys. Rev. Letters 21, 392 (1968).

In Fig. 3 we show four typical examples of anticlockwise Argand loops obtained from the partial-wave projection of the Regge-pole exchanges. They have shapes at least similar to, though much smaller than, those of the actual phenomenological phase-shift analysis.[13] Our Argand diagrams of the D_{13} and F_{37} states in Fig. 3 roughly agree with those obtained by Kohsaka *et al.*[5] We do not obtain loops as large as those obtained by Collins *et al.*[6] We suspect that this difference comes from the fact that Collins *et al.* used Rarita *et al.*'s Regge parameters[20] multiplied by an arbitrary factor $\sin\alpha(t)$ for the forward region. Rarita *et al.*'s parameters are not reliable in the large-$|t|$ region.

[20] W. Rarita, R. J. Riddell, Jr., C. B. Chiu, and R. J. N. Phillips, Phys. Rev. 165, 1615 (1968).

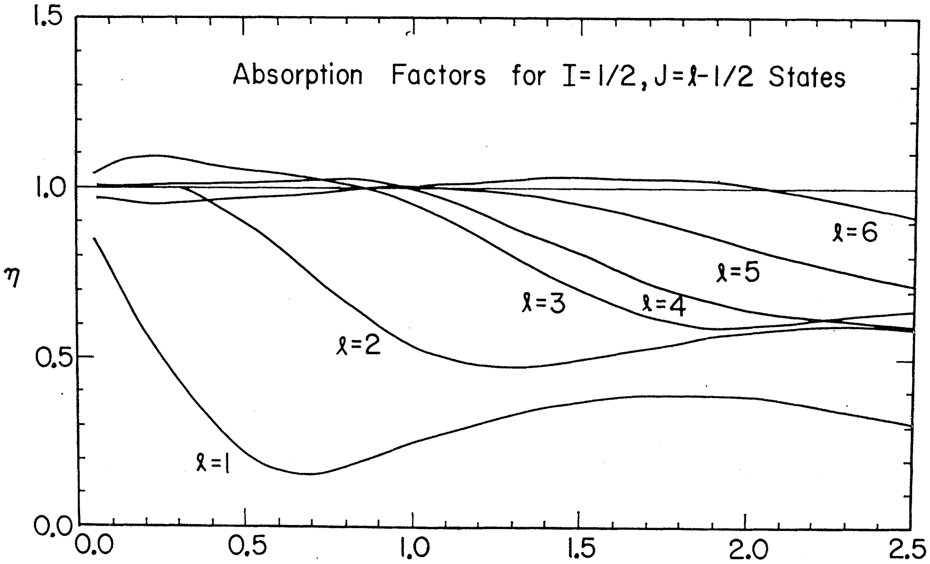

FIG. 6. Typical behavior of the absorption factors $\eta(W)$ obtained from the Regge-pole exchanges.

In Figs. 4 and 5 we show the corresponding $\delta_r(W)$ and $\eta(W)$. Also shown are the results of the phenomenological phase-shift analysis for $\delta_r(W)$ and $\eta(W)$ due to Bareyre *et al.*[13] *We* can see that the phase shift $\delta_r(W)$ from the Regge-pole exchanges behaves very smoothly, while the $\delta_r(W)$ of Bareyre *et al.* sharply increases near the resonance energy. The absorption factor $\eta(W)$ from the Regge-pole exchanges behaves smoothly also.

In Fig. 6 we explained the behavior of the absorption factors $\eta(W)$ in more detail. We see that the $\eta(W)$'s for the $l \geq 2$ partial-wave amplitudes violate the unitarity limit in the low-energy region, and that each decreases only as far as the asymptotic value. Therefore, this common behavior of $\eta(W)$ has no dynamical meaning related to the resonance.

In order to test whether these four anticlockwise Argand loops really correspond to cross-section peaks

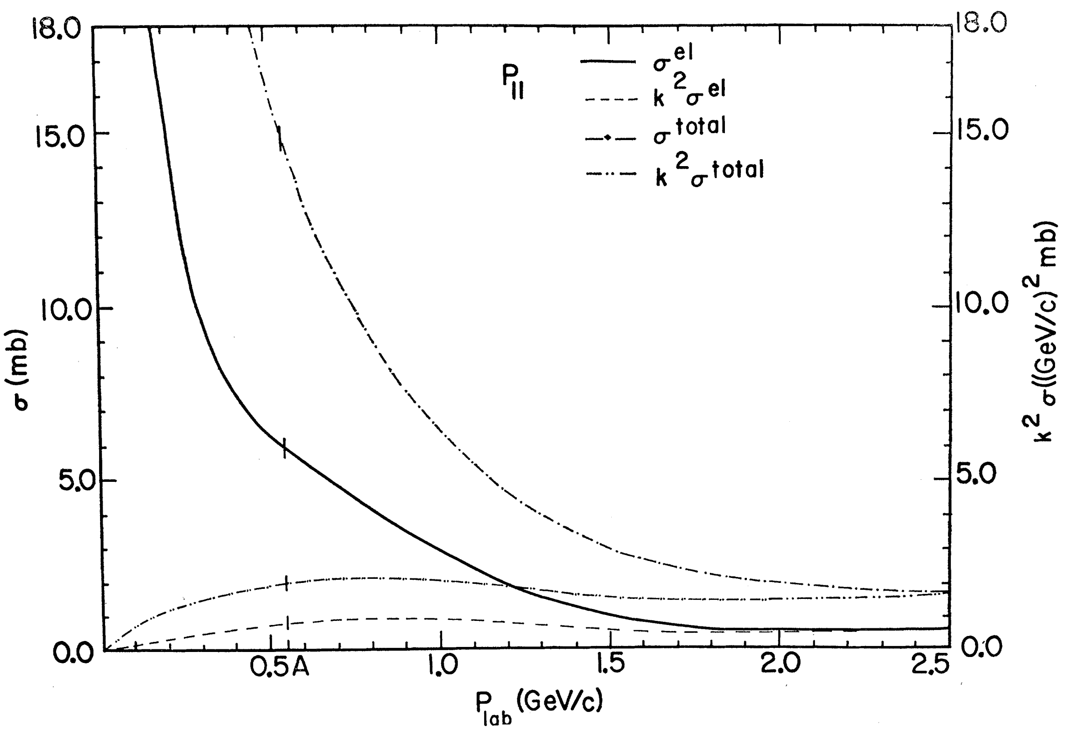

FIG. 7. Behaviors of $\sigma_{Jl}^{\text{tot}}(W)$, $\sigma_{Jl}^{\text{el}}(W)$, $k^2\sigma_{Jl}^{\text{tot}}(W)$, and $k^2\sigma_{Jl}^{\text{el}}(W)$ obtained from the Regge-pole exchanges in the P_{11} state.

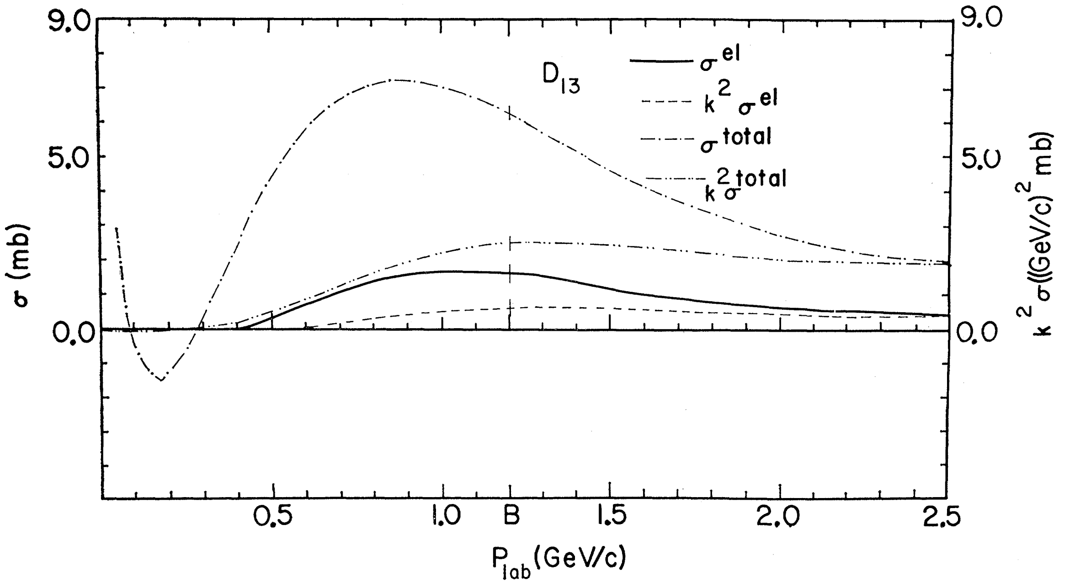

FIG. 8. Same as in Fig. 7 in D_{13} state.

or not, we computed the partial-wave total and elastic cross sections. We also computed $k^2\sigma_{Jl}^{tot}(W)$ and $k^2\sigma_{Jl}^{el}(W)$, which should at least exhibit the typical behavior corresponding to the anticlockwise Argand loops. These are shown in Figs. 7–10.

We discuss two cases. One is the P_{11} state, in which the absorption factor $\eta(W)$ satisfies the unitarity-limit requirement in all energy regions. Although the Argand diagram for the P_{11} state shows an anticlockwise loop very similar to that of Baryere *et al.*'s phenomenological one, both $\sigma_{Jl}^{tot}(W)$ and $\sigma_{Jl}^{el}(W)$ decrease monotonically and approach the asymptotic behavior as energy increases. Only $k^2\sigma_{Jl}^{tot}(W)$ and $k^2\sigma_{Jl}^{el}(W)$ show the very broad peaks. The above two facts indicate that these broad peaks in $k^2\sigma_{Jl}^{tot}(W)$ and $k^2\sigma_{Jl}^{el}(W)$ cannot be expressed by a Breit-Wigner-type resonance formula because the energy dependence of $k^2\sigma_{Jl}^{tot}(W)$ and $k^2\sigma_{Jl}^{el}(W)$ in Fig. 6 is much weaker than that of the Breit-Wigner formula. Of course, the experimentally observed resonances in this energy region have pronounced peaks in $\sigma_{Jl}^{tot}(W)$ and $\sigma_{Jl}^{el}(W)$ as well as in $k^2\sigma_{Jl}^{tot}(W)$ and $k^2\sigma_{Jl}^{el}(W)$.[13]

We can generally expect that if the absorption factor $\eta(W)$ in any partial-wave amplitude obtained from the Regge-pole exchange satisfies the unitarity limit in all energy regions, then the corresponding cross sections will show monotonic behavior similar to the P_{11} case. The broad peaks in $k^2\sigma_{Jl}^{tot}(W)$ and $k^2\sigma_{Jl}^{el}(W)$ in the momentum retion 0.5–1.0 GeV/c are simply turning points between the vanishing value of $k^2\sigma_{Jl}^{tot}(W)$ and $k^2\sigma_{Jl}^{el}(W)$ at the threshold and the asymptotic behavior at large k^2.

In the D_{13}, F_{15}, and F_{37} states, each absorption factor becomes larger than 1 in the low-energy region and thus

FIG. 9. Same as in Fig. 7 in F_{15} state.

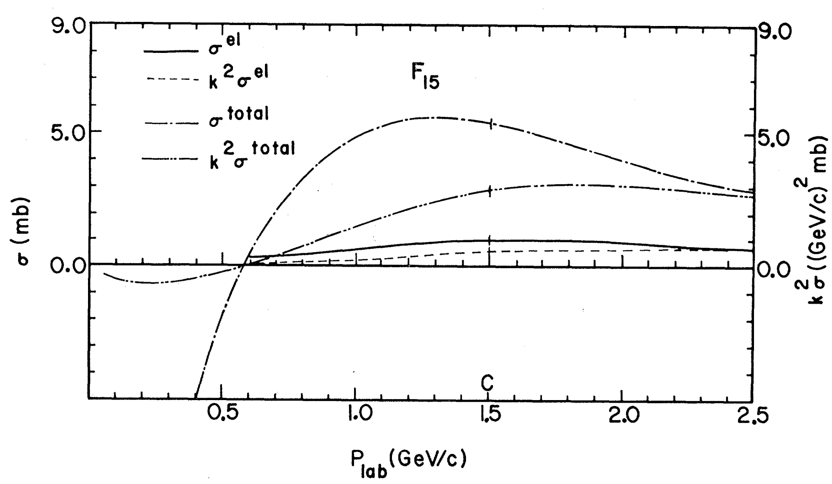

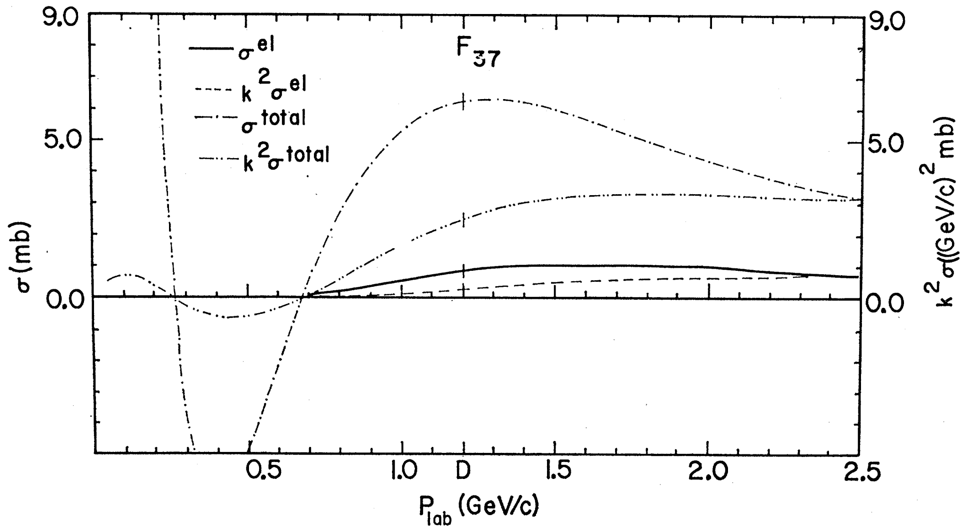

FIG. 10. Same as in Fig. 7 in F_{37} state.

violates unitarity. In this low-energy region, the total cross section becomes negative, as can be understood from Eq. (5). Considering the monotonically decreasing cross sections in the P_{11} state in which $\eta(W)$ satisfies the unitarity limit, it is evident that when $\eta(W)$ violates the unitarity limit in the low-energy region, $\sigma_{Jl}{}^{\text{tot}}(W)$ and $\sigma_{Jl}{}^{\text{el}}(W)$ produce broad peaks in the processes to reach the monotonically decreasing behavior in the high-energy region from the negative cross section in the low-energy region. This behavior of cross sections may be expected for all partial-wave amplitudes in which the absorption factors violate the unitarity limit. These broad peaks certainly have no connection with a Breit-Wigner-type resonance peak.

The important fact is that in the D_{13}, F_{15}, and F_{37} states both $k^2\sigma_{Jl}{}^{\text{tot}}(W)$ and $k^2\sigma_{Jl}{}^{\text{el}}(W)$ are almost constant over the momentum interval of width 0.7 GeV/c about the maximum points of Im$a_{Jl}(W)$ [see Fig. 14 for the maximum points of Im$a_{Jl}(W)$]. This fact indicates that the anticlockwise Argand loops obtained from the partial-wave projection of the Regge-pole exchanges essentially corresponds to the flat behavior of $k^2\sigma_{Jl}{}^{\text{tot}}(W)$ and $k^2\sigma_{Jl}{}^{\text{el}}(W)$ discussed in Sec. II. We thus conclude that there is no Breit-Wigner-type resonance peak in the partial-wave cross sections obtained from the Regge-pole exchanges.

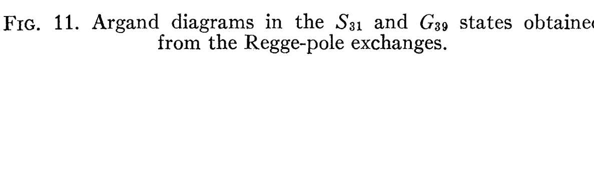

FIG. 11. Argand diagrams in the S_{31} and G_{39} states obtained from the Regge-pole exchanges.

If the anticlockwise Argand loop obtained from Regge-pole exchanges has no relation to the existence of the Breit-Wigner-type resonance peak, one may guess that the typical cross-section behavior so far discussed may also apply to partial-wave amplitudes which have no anticlockwise Argand loop.

In order to justify this observation, we show the Argand diagram, $\sigma_{Jl}{}^{\text{tot}}(W)$, $\sigma_{Jl}{}^{\text{el}}(W)$, $k^2\sigma_{Jl}{}^{\text{tot}}(W)$, and $k^2\sigma_{Jl}{}^{\text{el}}(W)$ for the S_{31} and G_{39} states obtained from the Regge-pole exchanges. As is shown in Fig. 11, these two partial-wave amplitudes have no anticlockwise Argand loop. However, the plotted cross-section behavior in S_{31} (see Fig. 12) is quite similar to that of the P_{11} state. Also the cross-section behavior of the G_{39} state is similar to that of the F_{15} and F_{37} states (see Fig. 13).

Although the Argand loci in our Figs. 3 and 11 are plotted up to 2.5 GeV/c, several partial-wave amplitudes, for example, P_{11}, draw a second anticlockwise loop as the momentum increases from 2.5 GeV/c.[21] The variation of $k^2\sigma_{Jl}{}^{\text{tot}}(W)$ and $k^2\sigma_{Jl}{}^{\text{el}}(W)$ due to the existence of the secondary anticlockwise loop above 2.5 GeV/c is extremely small and almost negligible. The variation of $\sigma_{Jl}{}^{\text{tot}}(W)$ and $\sigma_{Jl}{}^{\text{el}}(W)$ due to the above secondary anticlockwise loop is overcome by the kinematical factor $1/k^2$, and $\sigma_{Jl}{}^{\text{tot}}(W)$ and $\sigma_{Jl}{}^{\text{el}}(W)$ monotonically decrease with increasing energy. This situation is the same as in the first anticlockwise loop in the P_{11} state. We have already explained the reason why we cannot interpret the above anticlockwise Argand loop as an indication of a Breit-Wigner-type resonance, when $\sigma_{Jl}{}^{\text{tot}}(W)$ and $\sigma_{Jl}{}^{\text{el}}(W)$ decrease monotonically.

We show in Fig. 14 the partial-wave total-cross-section behavior over the momentum region 0–4.0 GeV/c for the six partial-wave amplitudes above. We can see that all $\sigma_{Jl}{}^{\text{tot}}(W)$ above 1.5 GeV/c show no

[21] The existence of such secondary loops is noted in several papers. See, for example, Ref. 11.

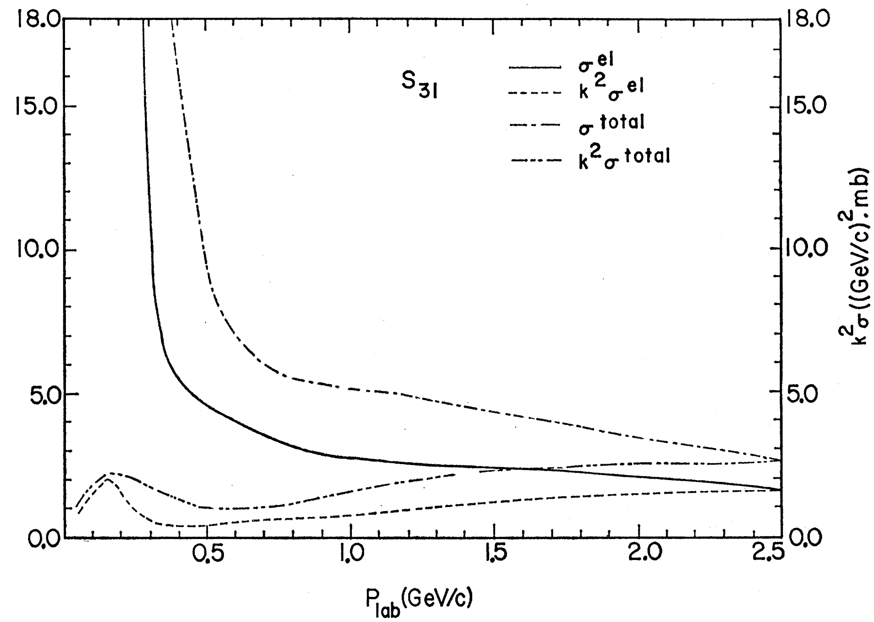

FIG. 12. Behavior of $\sigma_{Jl}^{tot}\times(W)$, $\sigma_{Jl}^{el}(W)$, $k^2\sigma_{Jl}^{tot}(W)$, and $k^2\sigma_{Jl}^{el}(W)$ obtained from the Regge-pole exchanges in the S_{31} state.

structure, even though some states such as the P_{11}, F_{15}, and F_{37} have a maximum of $\mathrm{Im}\,a_{Jl}(W)$.

We have explained that, in the P_{11} state, the variation of the cross section due to the anticlockwise Argand loop is extremely small. Therefore, although the effect of the existence of an anticlockwise Argand loop may appear in $k^2\sigma_{Jl}^{tot}(W)$ as a broad peak, it does not appear in $\sigma_{Jl}^{tot}(W)$, because the kinematical factor $1/k^2$ in $\sigma_{Jl}^{tot}(W)$ overcomes the variation due to the anticlockwise Argand loop. As was explained in Sec. II, if we assume a Breit-Wigner-type resonance for a cross-section peak, $\sigma_{Jl}^{tot}(W)$ should also have a peak unless the corresponding energy is very close to the elastic threshold. However, we see in Fig. 14 that $\sigma_{Jl}^{tot}(W)$ in the P_{11} state monotonically decreases and that $\sigma_{Jl}^{tot}(W)$ in other states also monotonically decrease after they reach a maximum starting from negative cross sections due to the violation of unitarity.

In this section we have shown that Schmid's interpretation of the partial-wave projection of the Regge-pole exchanges as the direct-channel resonance is wrong. We also dispute the statement of Collins *et al.*

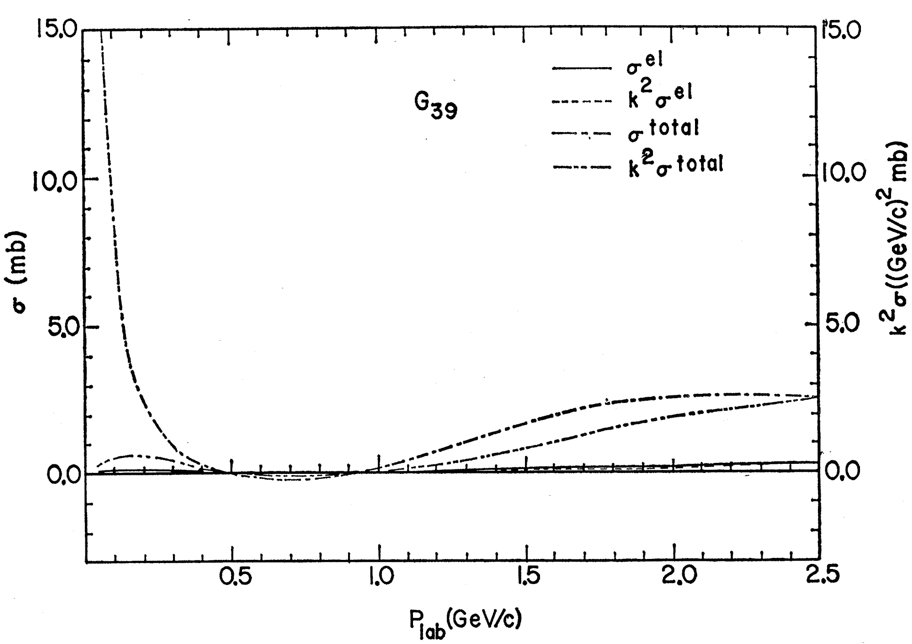

FIG. 13. Same as in Fig. 12 in the G_{39} state.

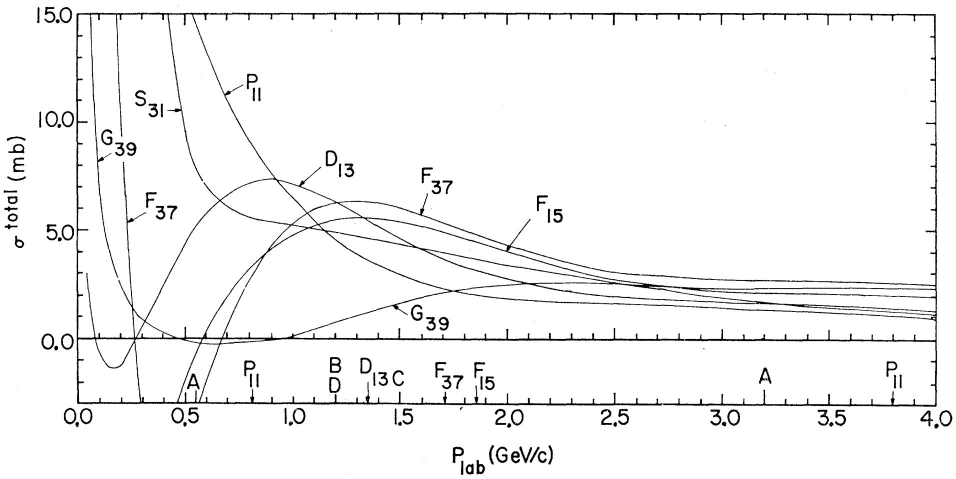

FIG. 14. Typical behavior of $\sigma_{Jl}^{tot}(W)$ obtained from the Regge-pole exchanges in the momentum region 0–4.0 GeV/c. The points A, B, C, and D have the same meanings as in Fig. 3. The maximum points of $\mathrm{Im}a_{Jl}(W)$ in the anticlockwise Argand loops in the P_{11}, D_{15}, F_{15}, and F_{37} are indicated by arrows. Notice that there is no cross-section peak either at the $\delta_r(W)=0$ points (i.e., A, B, C, and D) or at the maximum points of $\mathrm{Im}a_{Jl}(W)$.

that the resonating partial-wave amplitudes obtained from Regge-pole exchanges are canceled by other nonresonating partial-wave amplitudes so as to give smooth behavior for the total amplitudes. Since all partial-wave amplitudes have essentially the same behavior, independent of the existence of the anticlockwise Argand loops in certain partial waves, no such cancellation occurs.

In conclusion, we stress that the anticlockwise loops obtained from Regge-pole exchanges have no relation to the direct-channel resonances, contrary to Schmid's statement. We interpret these anticlockwise loops as the ones which are characteristic of the Regge-pole model, as suggested in Ref. 11, because the cross sections obtained from Regge-pole exchanges simply show the characteristics of the background amplitude (i.e., smooth behavior). The broad peak at low energy when $\eta(W)$ violates unitarity is simply caused by $\eta(W)$ and the kinematical factor $1/k^2$ in Eq. (5).

IV. CONCLUDING REMARKS

In Sec. III we showed that the partial-wave cross sections obtained from Regge-pole exchanges do not show any resonancelike behavior even though certain partial-wave amplitudes have anticlockwise Argand loops. We showed that all partial-wave cross sections thus obtained from the Regge-pole exchanges have essentially the same behavior independent of the shape of the Argand loops.

Schmid's interpretation of the anticlockwise Argand loops obtained from the Regge-pole exchanges as the direct-channel resonance is not correct.

Under these circumstances, it is important to clarify the meaning of the duality principle. As has been pointed out, the concept of strong duality is very ambiguous.[12]

In our present paper, we further showed that as far as Schmid's interpretation is concerned, strong duality[12] is not correct, because the partial-wave projection of Regge-pole exchanges does not give rise to any resonancelike cross section.

Although Schmid[17] insists that Regge-pole exchange is the force which produces a resonance pole in the N/D-type equation from the point of view of the duality principle, we have already shown that Regge-pole exchange is not the force which produces the resonance pole in an N/D-type equation.[22] The attractive force obtained from Regge-pole exchanges is always too weak to produce a resonance in the dynamical calculation. This fact is amply shown in our Figs. 4 and 5.

As for the description of the intermediate-energy pion-nucleon scattering, we[15] have recently shown that the interference model, in which the Regge-pole exchanges and the Breit-Wigner resonance formula with complex phase factors from Regge-pole exchanges are added, can fit the experimental data more satisfactorily than any other models.[15]

The failure of the fit of the π^+p backward scattering has been cited by many critics[2] of the interference model because the interference model shows severe double counting. However, it has recently been pointed out that the baryon Regge-pole parameters used in the above calculation are probably not the correct ones,[23] because these baryon Regge-pole parameters cannot reproduce the new π^+p polarization data at 2.75 GeV/c.[24]

Schmid[17] also says that the anticlockwise loops obtained from Regge-pole exchanges and those of the

[22] N. Masuda, Phys. Rev. **175**, 2087 (1968).
[23] R. Odorico, Nuovo Cimento Letters **2**, 1 (1969).
[24] R. J. Esterling *et al.*, in *Proceedings of the Fourteenth International Conference on High-Energy Physics*, edited by J. Prentki and J. Steinberger (CERN, Geneva, 1968), Fig. 38, p. 348.

Breit-Wigner formula should not be added. But from our numerical results, we can say that to add the two kinds of anticlockwise loops produces no difficulty since the partial-wave cross sections obtained from the Regge-pole exchanges exhibit essentially the characteristic of nonresonant behavior except in the unitarity-violating threshold region as is shown in Figs. 7–10 and 14. In this connection we note that the variation of the Argand locus with respect to energy obtained from the Regge-pole exchanges is extremely weak compared to that of a phenomenological phase-shift analysis. This fact means that even when we add the anticlockwise loop obtained from Regge-pole exchanges to that of the Breit-Wigner amplitude, it produces only a small modification in the latter loop.

ACKNOWLEDGMENT

The author would like to express his sincere thanks to E. Carriere for his help in improving the manuscript.

PHYSICAL REVIEW D VOLUME 1, NUMBER 9 1 MAY 1970

Lepton-Hadron Deep-Inelastic Scattering, Gluon Model, and Reggeized Symmetry Breaking*

RICHARD A. BRANDT† AND GIULIANO PREPARATA‡
Rockefeller University, New York, New York 10021
(Received 8 December 1969)

We numerically estimate the expectation value between baryons of the equal-time commutator $[\dot{J}_i^a, J_j^b]$ of $U(3)\otimes U(3)$ currents on the gluon model by using a symmetry-breaking theory based on Regge-pole dominance. The result is in excellent agreement with the electroproduction data.

THE scaling behavior predicted by Bjorken[1] for deep-inelastic electron and neutrino scattering from hadrons has received considerable experimental support.[2–4] One of the most interesting consequences of scaling is the Callan-Gross[5] relation between certain integrals of the electroproduction structure functions and the infinite-momentum limit of the commutator $[\dot{J}_i(x),J_j(0)]\delta(x_0)$ of electromagnetic currents. The relation therefore enables one to determine which models for this commutator are in agreement with experiment. The recent experimental results[2–4] are in agreement with models in which the constituents of J_μ have spin $\frac{1}{2}$ and seem to be in disagreement with other models. We therefore propose in this paper to take a spin-$\frac{1}{2}$ model seriously and try to evaluate *numerically* matrix elements of current commutators by making some reasonable assumptions about the way in which the $\frac{1}{2}^+$ baryon octet deviates from an exactly $SU(3)$-symmetric multiplet. We find the resulting (generalized) Callan-Gross relation to be in excellent agreement with experiment.

The model we shall study is the so-called gluon model with Hamiltonian density[6]

$$\mathcal{H}=\psi^\dagger(-i\boldsymbol{\alpha}\cdot\nabla+\beta M+g\beta\gamma^\mu B_\mu)\psi+\mathcal{H}_B\,, \tag{1}$$

where ψ is a spin-$\frac{1}{2}$ quark field, B_μ is a neutral vector meson, $\mathcal{H}_B$ is the Hamiltonian of B_μ, and[7]

$$M=\alpha_0\lambda^0+\alpha_8\lambda^8 \tag{2}$$

is the quark mass term. Thus the chiral $SU(3)\otimes SU(3)$ symmetry breaking is due entirely to the explicit quark mass term. It is the very smooth nature of this symmetry-breaking mechanism which will enable us to proceed.

It is perhaps appropriate to mention that this model has already been shown to have very desirable features in problems connected with radiative corrections to weak interactions[8] and nonleptonic weak interactions.[9]

The $U(3)$ vector currents are given in the gluon model by

$$J_\mu{}^a=\tfrac{1}{2}\bar{\psi}\gamma_\mu\lambda^a\psi\,,\quad a=0,\,\ldots,\,8. \tag{3}$$

We can write, in general, that

$$-\int d^4x\,\delta(x_0)\langle p|[\dot{J}_i{}^a(x),J_j{}^b(0)]|p\rangle \equiv iE^{ab}p_ip_j+\bar{R}^{ab}\delta_{ij}+G^{ab}\epsilon_{ijk}p_k\,, \tag{4}$$

* Supported in part by the Air Force Office of Scientific Research under Grant No. AF-AFOSR-69-1629.

† A. P. Sloan Foundation Fellow, on leave from University of Maryland.

‡ Fulbright Scholar.

[1] J. D. Bjorken, Phys. Rev. **179**, 1547 (1969).

[2] E. D. Bloom *et al.*, Phys. Rev. Letters **23**, 930 (1969); M. Breidenbach *et al.*, *ibid.* **23**, 935 (1969).

[3] W. Albrecht *et al.* (unpublished).

[4] I. Budagov *et al.*, Phys. Letters **30B**, 364 (1969).

[5] C. Callan and D. J. Gross, Phys. Rev. Letters **22**, 156 (1969).

[6] In the following we use (1) in a formal way along with canonical commutation relations, ignoring all perturbation-theoretic subtleties.

[7] We use the λ matrices of M. Gell-Mann, Phys. Rev. **125**, 1067 (1962); in particular, $\lambda_0=(\frac{2}{3})^{1/2}1$.

[8] C. Callan, Phys. Rev. **169**, 1175 (1968); G. Preparata and W. I. Weisberger, *ibid.* **175**, 1965 (1968).

[9] S. Nussinov and G. Preparata, Phys. Rev. **175**, 2180 (1968).